Hydroprocess2023 | 14th International Conference on Process Hydrometallurgy

New method to design and project behavior of a heap under simultaneous irrigation and aeration conditions

J. Menacho[1]* and G. Vega[2]

1. *De Re Metallica Ingeniería SpA, Chile, Gerente General, Jorgemenacho@drm.cl*
2. *De Re Metallica Ingeniería SpA, Chile, Ingeniero de Procesos, Guillermo.vega@drm.cl*

ABSTRACT

This paper in focused in the fluid dynamic design and optimization of copper sulphide heap leaching operations, where simultaneous irrigation and aeration are applied.

The first step to get the appropriate results, deals with the selection of samples that represent the physical characteristics of the units in the orebody to be leached. The best samples are the "massive" ones, but when this is not possible, a procedure, based on comminution principles, must be used.

Then agglomeration tests are conducted to set acid and water dosage. The acid dosage is chosen as a given percent of the analytical acid consumption and the water dosage is based on the shrinkage Atterberg limit, that is, the amount of water over which the bed is not expanded anymore (modified ASTM D4943). Then, controlled hydraulic and pneumatic conductivity tests are conducted to verify compatibility between irrigation and aeration rates. These tests are performed under controlled conditions, providing information to design and optimize the irrigation and the aeration calendar.

Results are interpreted using the infiltration theory of two fluids counter currently moving throughout a porous bed under variable saturation conditions, such occur in real sulphide heap leaching operations.

A case study is presented, which describes the stages of experimentation, scaling of results and simulation of the industrial heap under different irrigation and aeration conditions. This mineral crushed to a P80 of 1/2 "with 12% -100#, stacked at 6 m height, supports an irrigation rate of 8 L/h/m^2, producing 61% liquid saturation still suitable for 0.10 Nm^3/h/m^2. The same heap elevated to 8 m, produces liquid saturation over 70%, with insufficient aeration and possible channeling of the air. If 10 m are now considered, not only aeration become limited but also static liquefaction may occur because liquid saturation overpass 80%.

INTRODUCTION

Motivation: Chloride leach of copper sulphides

Leaching of low-grade sulphide ores requires counter current irrigation of solution and simultaneous air application. At any leaching scheme, air is always the ultimate oxidant agent. Net reaction for chloride leaching of chalcocite is as follows:

$$Cu_2S + \underbrace{O_2}_{\text{Aeration}} + \underbrace{4H^+ + 8Cl^-}_{\text{Irrigation}} \rightleftarrows 2CuCl_4^{2-} + S + 2H_2O$$

Assuming one ton of ore containing 0.5% CuT as chalcocite, for 80% recovery we need 6.13 kg/t H_2SO_4 and 4.67 Nm^3/t of air. Considering half of this copper is dissolved during the initial curing and repose step, the theoretical aeration rate in the first 30 days is 0.065 $Nm^3/h/m^2$. For a pad height of 10 m and 1.65 t/m^3 ore density we can assume a reasonable 25% consumption from the aeration rate, then 0.065/0.25 = 0.26 $Nm^3/h/m^2$ is the recommended flowrate during the initial 30 days. Once the irrigation proceeds, the air flowrate is planned to reduce to 0.13 $Nm^3/h/m^2$ until the end of the 150 days of irrigation. Clearly, the air inflow can be measured at the blower entrance, but distribution is a different issue.

The first question is how can we be sure that 0.26 $Nm^3/h/m^2$ may effectively cross upward the 10 m pad when different physical quality ores are fed?

After the 30 days of repose, the pad is subjected to 7 days wetting with a variable on/off irrigation calendar and finally, the liquid inflow is fixed in 8 $L/h/m^2$ for about 150 days.

How can we anticipate whether 0.13 $Nm^3/h/m^2$ of air move up when liquid is moving down at 8 $L/h/m^2$? What would happen when the physical quality of the ore become worse?

In this paper, we present a methodology aimed to answer the above-mentioned questions as well as the systematic design of industrial irrigation and aeration systems.

METHODOLOGY

Fluid dynamic infiltration through porous bed

As the aqueous solution is steadily added to the dry ore, first the surface of the particles start wetting, as moisture increases pendular water bridges link individual particles. This is the residual zone where the water phase is discontinuous, firmly bound to the particle skeleton, while the air moves freely. Then funicular blots grow at different regions in the porous bed, more and more particles are added into the network of liquid, and eventually all clusters get into contact at a given transition point, known as the cohesion peak. The liquid now exists as a continuous phase even it is far below full saturation (Soltani et al., 2021).

Further irrigation leads to overpass the critical saturation zone, when the liquid starts moving as a continuous phase. This originates the capillary flow regime and the first liquid exit is known as the pad leakage point.

The cohesion peak divides the funicular regime into two sub regions, namely, the ascending cohesion in the earlier funicular regime and the descending cohesion in the late funicular regime, when an increasing number of pores reach high saturation level and the soil suction is strongly reduced.

Further increase in the liquid content produces increasing liquid permeability, which becomes maximum when the complete saturation is reached. At the air entry point or even below it, the gas flow is interrupted and air permeability is negligible.

Modelling frame

The SWCC curve reaches a steady region where the water suction reduces linearly (in log scale) with the increasing liquid saturation. The air conductivity is often strongly reduced, even if the saturation is below the air entry point, and it is related to the increasing number of air trajectories now clogged with liquid, the internal air becomes stagnant within the liquid network. The heavier and more viscous liquid can displace the lighter and thinner air, but not the reverse. The air inflow is a conditioned input variable.

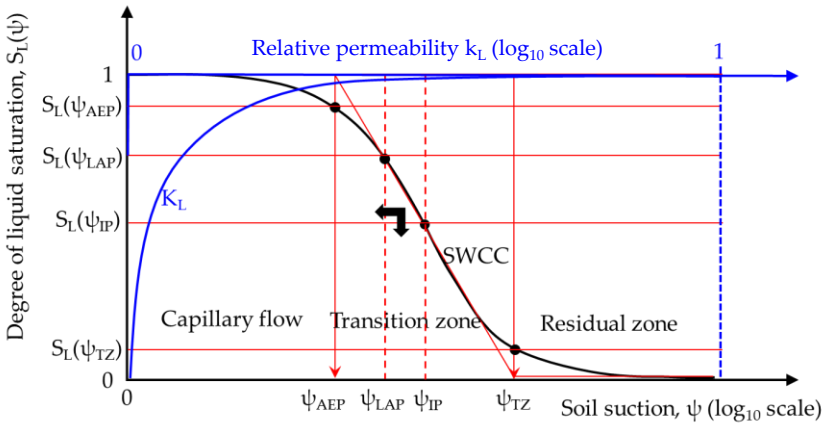

Figure 1 Soil water characteristic curve and the liquid reduced permeability

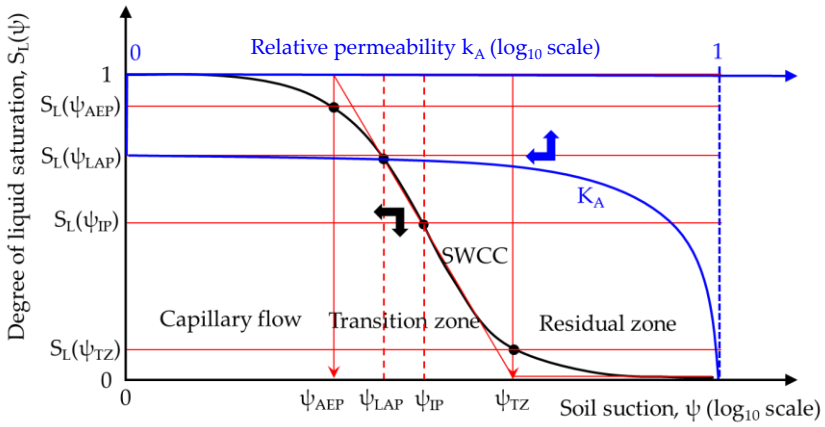

Figure 2 Soil water characteristic curve and the pneumatic reduced permeability

Liquid and air numerical simulation

Air behaves as a compressible fluid whose density changes significantly with a change in air pressure or temperature. The advection flow of air through an unsaturated soil commences as the air phase becomes continuous. When the degree of saturation is near the air entry point, the air phase exists as occluded air bubbles and air flow is then reduced to diffusion and advection, not considered in this formulation.

First, the Richards equation for the liquid is solved assuming the initial saturation, the irrigation vector as well as the hydraulic conductivity function are known. The Richards equation for the air flow is then solved to calculate the admissible air flow according to the liquid saturation condition computed between t and t + Δt. The effective porosity, the air conductivity curve and temperature need to be known. Flows are corrected by temperature according to the ideal gas law. The admissible air flow is always the upper limit to the actual air flow. The air outflow is computed as a fraction of the air inflow. Iteration proceeds until reaching the total process time. Hydrodynamic and pneumatic efficiency indices are also computed. Main equations are described below.

Water flow is partially saturated media (Kim Y.S. et al., 2013):

$$q_w = K_w\left(S_w, t\right)\left[-\frac{\partial p_w}{\partial t} + \varrho^{wR} g\right] \tag{1}$$

Hydraulic conductivity curve (van Genuchten M.T., 1980):

$$K_w\left(S_w\right) = K_{ws}\, S_w^{0.5}\left[1-\left(1-S_w^{1/m}\right)^m\right]^2 \tag{2}$$

Air flow in partially saturated media (Coussy O., 2004):

$$q_a = K_a\left(S_a, t\right)\left[-\frac{\partial p_a}{\partial t} + \varrho^{aR} g\right] \tag{3}$$

Pneumatic conductivity curve (this work):

$$K_a\left(t\right) = K_{as}\left[1 - \left(S_w\left(t\right)/S_{wap}\right)^{\phi_a}\left\{1 - \left[1 - \left(S_w\left(t\right)/S_{wap}\right)^{1/m_a}\right]^{m_a}\right\}^2\right], S_{wr} \le S_w\left(t\right) \le S_{wap} \tag{4}$$

Air volume correction by temperature (ideal gas law):

$$p_a \frac{dV_a}{dt} = n_a R \frac{dT_a}{dt} \tag{5}$$

Experimental fluid dynamic test

Experimental system to measure hydraulic and pneumatic conductivity curves as well as controlled leaching test aimed to check relationship between liquid and air flowrate for different physical quality ores is shown in Figure 3.

Figure 3 Arrangement for fluid dynamic testing. Photo courtesy of ProExito Laboratory. The only lab in Chile offering fluid dynamic test with controlled irrigation and aeration conditions

Results and interpretation

Figure 4 shows the particle size distribution of the sample and Figure 5 shows the SWCC profile deduced from pedotransfer function according to Fredlund, and validated with the hydrodynamic test results.

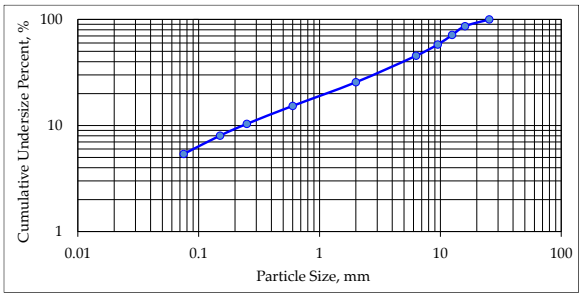

Figure 4 Test ore sample, P80 = 14.5 mm and 8.01% -100#. 61.71% gravel, 32.91% sand and 5.37% clays.

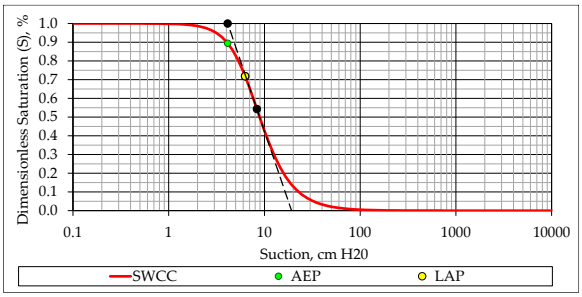

Figure 5 SWCC estimated from the PSD and validated with the column liquid balance. AEP = 4.14 cm H_2O, S = 89.4%. LAP = 6.28 cm H_2O, S = 71.9%.

Figure 6 shows experimental influent and modelled effluent. Figure 7 shows experimental and modelled air influent while Figure 8 shows the variogram of the modelled liquid saturation along the time. Finally, Figure 9 shows experimental and modelled hydraulic and pneumatic conductivity curves. Agreement is generally reasonable.

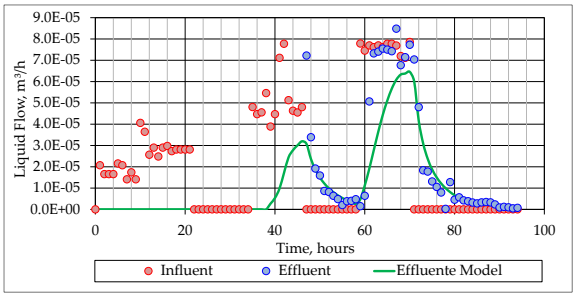

Figure 6 Experimental and modelled liquid influent and effluent

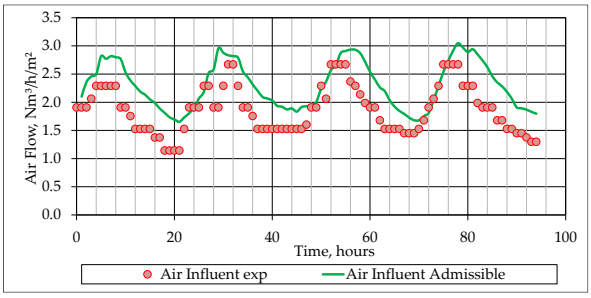

Figure 7 Experimental and modelled air influent and maximum admissible air flow

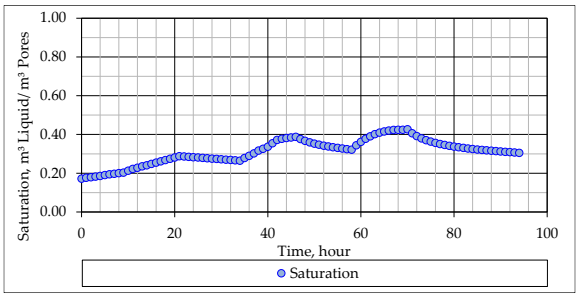

Figure 8 Evolution of liquid saturation along the time

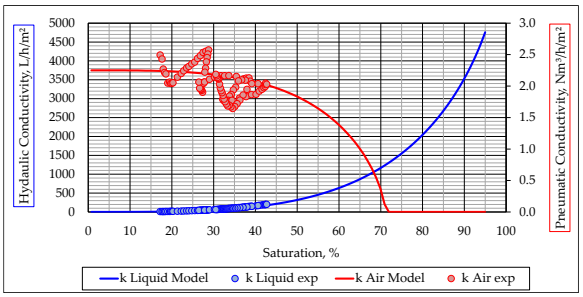

Figure 9 Hydraulic and pneumatic conductivity curves. Point are experimental and lines are modeled

Projection to industrial heap leaching

Figure 10 shows simulation of the liquid saturation along a chloride heap leaching cycle, with an initial 30-day repose, followed by 2 cycles of irrigation and 14-day of repose and a final wash with acid water and a 7-day drainage step. The exercise was run for 6, 8 and 10 L/h/m². Initially saturation diminishes due to drying by the air. Saturation increases as the irrigation rate increases. Saturation increases along the time due to loss of permeability.

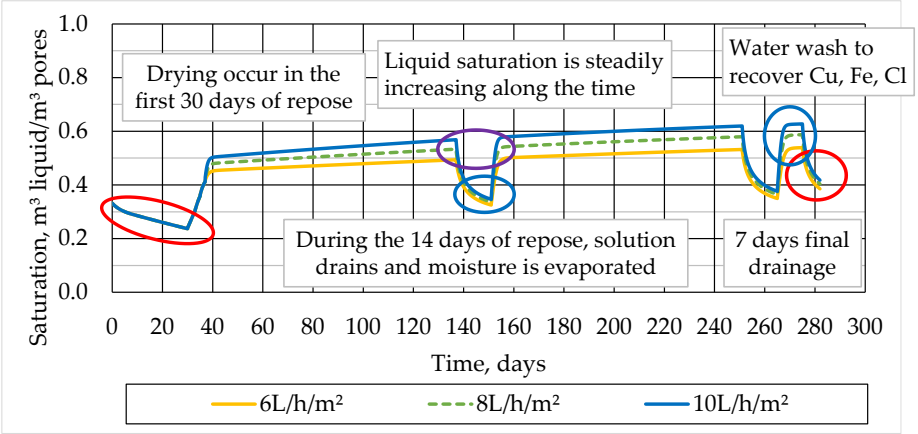

Figure 10 Simulation of chloride leaching: repose/irrigation cycles, under aeration. Pad height = 6m, 12%-100#

Figure 11 shows the admissible air flowrate along the time. Response is inversely proportional to the liquid saturation evolution. Applied air inflow should be always less than the admissible one, otherwise, the air will be channeled and part will leave by the slopes and the lower sides of the pad.

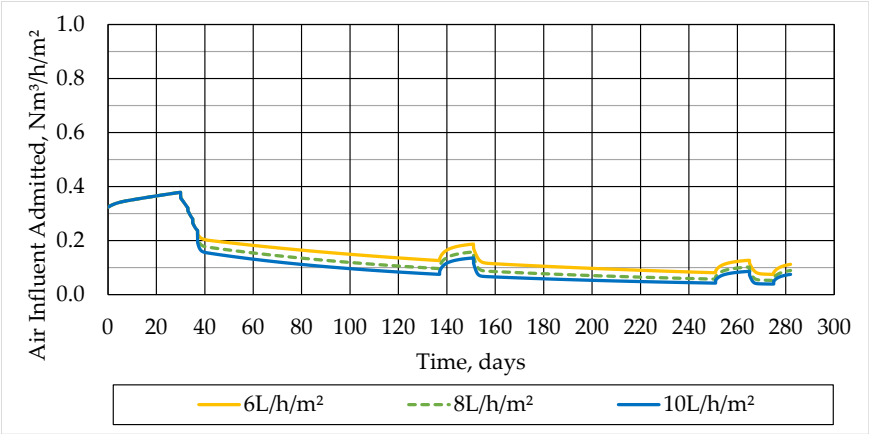

Figure 11 Change in the admissible air flow along the time. 6m pad height, 12%-100#.

Table 1 summarizes simulations to select optimal conditions. Aeration needs saturation < 65% while irrigation needs saturation < 75%, to comfortable operate a pad 6 m height, continuously irrigated with 8 L/h/m², aerated at 0.10 Nm³/h/m² and the ore with 12% -100#. The green color indicates saturation < 65%; yellow indicates saturation between 65% and 70%; orange indicates saturations between 70% and 75%; and red indicates saturation over 75%.

Table 1 Decision table: Irrigation rate - pad height - fines level. Planned air flowrate = 0.10 Nm³/h/m²

Height	Fines	KLiqSat	KAirSat	Liquid irrigation rate		
m	-100#	m/s	m/s	6 L/h/m²	8 L/h/m²	10 L/h/m²
4 m	8%	3.25.E-03	1.22.E-03	46.0%	49.3%	52.0%
	12%	2.13.E-03	7.99.E-04	49.5%	53.1%	56.0%
	16%	1.49.E-03	5.59.E-04	50.6%	54.6%	58.0%
6 m	8%	1.80.E-03	6.77.E-04	51.8%	56.1%	59.6%
	12%	1.18.E-03	4.43.E-04	53.9%	58.7%	62.7%
	16%	8.27.E-04	3.10.E-04	60.5%	65.7%	69.9%
8 m	8%	1.11.E-03	4.16.E-04	62.9%	68.3%	72.8%
	12%	7.26.E-04	2.72.E-04	66.6%	72.6%	77.5%
	16%	5.08.E-04	1.91.E-04	70.2%	76.7%	81.9%
10 m	8%	7.17.E-04	2.69.E-04	71.8%	78.7%	84.5%
	12%	4.69.E-04	1.76.E-04	76.6%	84.0%	90.1%
	16%	3.29.E-04	1.23.E-04	80.4%	88.3%	94.6%

Conclusions

- A comprehensive procedure, experimental and theoretical, is now available in Chile to measure and estimate all parameters necessary to project fluid dynamic in irrigated and aerated heap leaching. Applicability of the developed tool is validated.
- The samples to conduct the tests not only must be geologically representative, but also need to be correctly prepared such that the size distribution represents the expected situation at the plant. This is particularly delicate when drilling core samples are considered. If this fail, the next hydrodynamic and pneumatic characterization is biased.
- The fluid dynamic test itself start fixing the aeration condition, flowrate, pressure and temperature. Then an irrigation ramp is applied with at least three flow steps. Once stabilization is reached at each step, liquid on-off flowrates are registered as well as the dynamic liquid content, also the reactive air flowrate, pressure and temperature are registered.
- Data is interpreted using the liquid and air flow dynamic model, based on the Richards equation, parameters are estimated and conveniently scaled to industrial conditions.
- Additional edometric consolidation data allows to predict the response of the heap at different height, operated with different liquid and aeration flowrates.

ACKNOWLEDGEMENTS

We acknowledge our clients to give us the opportunity to link hydrodynamics to metallurgy to understand what is Hydrometallurgy.

NOMENCLATURE

ψ_{AEP}	Matrical suction at air entry point
ψ_{LAP}	Matrical suction at liquid air plug
ψ_{IP}	Matrical suction at inflection point
ψ_{TZ}	Matrical suction at transition zone
k_A	Air permeability
k_L	Liquid permeability
q_w	Liquid infiltration rate
K_w	Hydraulic conductivity
K_{ws}	Saturated hydraulic conductivity
S_w or S_L	Liquid saturation (filling fraction of effective porosity)
t	Time
p_w	Liquid pore pressure
ϱ^{wR}	Density of the liquid
g	Gravitational acceleration constant
m	Constant in the van Genuchten model
q_a	Air infiltration rate

K_a	Pneumatic conductivity
K_{as}	Saturated air conductivity
S_a	Air saturation
p_a	Air pore pressure
ϱ^{aR}	Density of the air
S_{wap}	Liquid saturation over which air convection is negligible
ϕ_a	Constant in the air conductivity model
m_a	Constant in the air conductivity model
R	Universal constant for ideal gases
n_a	Number of moles of air
V_a	Volume of air
T_a	Air temperature

REFERENCES

Coussy O. (2004), '*Poromechanics*', 1st edition, John Wiley & Sons, New York, USA, (pages 45–51, 157–168)

Fredlund, D. G., & Xing, A. (1994). 'Equations for the soil-water characteristic curve'. *Canadian Geotechnical Journal*, Volume 31, Issue 4, pages 521-532.

Kim Y.S., Jaehong K., (2013) 'Coupled Hydromechanical Model of Two-Phase Fluid Flow in Deformable Porous Media', *Mathematical Problems in Engineering*, Hindawi Publishing Corporation, Volume 2013, Article ID 589452, 8 pages , (viewed 07/28/2023, http://dx.doi.org/10.1155/2013/589452).

Richards L.A., (1931) 'Capillary conduction of liquids through porous mediums', *Physics*, Volume 1, Issue 5, pages 318–333, (viewed 07/28/2023, https://doi.org/10.1063/1.1745010).

Soltani A., Azimi M., Boroomandnia A., O'Kelly B.C. (2021). 'An objective framework for determination of the air-entry value from the soil–water characteristic curve', *Results in Engineering*, Volume 12, 100298, (viewed 07/28/2023, https://doi.org/10.1016/j.rineng.2021.100298).

Van Genuchten M.T. (1980), 'Closed-form equation for predicting the hydraulic conductivity of unsaturated soils', *Soil Science Society of America Journal*, Volume 44, number 5, pages 35–53.